Design and NMR Characterization of Active Analogues of Compstatin Containing Non-Natural Amino Acids

Buddhadeb Mallik,[†,‡] Madan Katragadda,[‡,§] Lynn A. Spruce,[§] Caterina Carafides,[§] Christos G. Tsokos,[§] Dimitrios Morikis,*[,†] and John D. Lambris*[,§]

Department of Chemical and Environmental Engineering, University of California at Riverside, Riverside, California 92521, and Department of Pathology and Laboratory Medicine, University of Pennsylvania, Philadelphia, Pennsylvania 19104

Received June 8, 2004

We present new findings in our drug discovery effort to develop an anticomplement therapeutic. We have designed several active analogues of compstatin by altering its amino acid composition at positions 4 and 9. The most effective analogues have tryptophan or fused-ring non-natural amino acids at position 4 and alanine or an unbranched single-methyl amino acid at position 9. Twenty-one of these analogues have 2−99-fold higher activities compared to the parent peptide compstatin. The analogue Ac-V4(2Nal)/H9A-NH_2 has the highest inhibitory activity with IC_{50} 500 nM. NMR data, through NOE and chemical shift analysis, suggest the presence of interconverting conformers spanning the extended and helical regions of the Ramachandran plot, and they detect a predominant averaged conformer with coil structure and at least one flexible β-turn, of type I. The fused-ring non-natural amino acids at position 4 contribute to the formation of the hydrophobic cluster of compstatin, which has been previously proposed, together with the β-turn and a disulfide bridge, to be essential for binding to the target of compstatin, complement component C3. We propose that additional mechanisms may contribute to the structural stability of the analogues and to binding to C3, involving intra- and intermolecular electrostatic interactions of the π-electron system of side chain aromatic rings. The presence of $\pi-\pi$ interactions for Trp4−Trp7 was confirmed with a molecular dynamics simulation for the most active analogue with natural amino acids, Ac-V4W/H9A-NH_2. Alanine or aminobutyric acid at position 9 contribute to the weak propensity for helical structure of the residue segment 4−10 of the analogues, which may also play a role in increased activity.

Introduction

Compstatin is a 13-residue peptide that inhibits the activation of the complement system[1−3] and is a candidate to become a therapeutic agent (reviewed in refs 4−8). Compstatin binds to complement component C3 and blocks the cleavage of C3 to C3a and C3b, thus blocking the opsonic and inflammatory actions of C3 fragments and their contributions in B and T cell immune response. It also blocks the propagation of the complement activation pathways beyond C3, which results in the cell lysis membrane attack complex. C3 is the converging protein of the three known complement activation pathways, the classic, the alternative, and the lectin pathways.[9] Regulation of complement activation is necessary when the complement system fails to recognize "self" from "nonself" and attacks the host tissues. Unregulated complement activation is present in a variety of pathological conditions or in interventions to restore physiological conditions, such as many autoimmune diseases, burn injuries, trauma, stroke, transplantation, ischemia reperfusion injuries, cardiopulmonary bypass, and dialysis.[10−12] Compstatin was discovered by screening a phage-displayed random peptide library for binding to C3b[13] and has been tested in a variety of experiments and models in vitro, in vivo, and ex vivo.[13−24]

The sequence of compstatin is Ile1-[Cys2-Val3-Val4-Gln5-Asp6-Trp7-Gly8-His9-His10-Arg11-Cys12]-Thr13-NH_2, with the disulfide bond between Cys2 and Cys12 denoted by brackets. Early nuclear magnetic resonance (NMR) spectroscopy studies showed averaging of NMR observables, suggesting conformational averaging in compstatin.[25] NMR in combination with computational studies was used to determine the structure of a major conformer of compstatin, which consisted of a closed-loop coil with a type I β-turn opposite to the disulfide bridge and two residues (Ile1 and Thr13) hanging outside the closed loop.[25,26] The β-turn comprised residues Gln5-Asp6-Trp7-Gly8. The surface of compstatin is partitioned to a predominantly hydrophobic part (cluster) that includes the disulfide bridge and a predominantly polar part that includes the β-turn. The population of the major conformer of compstatin was estimated to be 42−63%, using NMR $^3J_{HN-H\alpha}$-coupling constant data.[25]

Molecular dynamics simulation studies based on the NMR structures confirmed that the major conformer of compstatin was a coil with a type I β-turn of population 44%, but it revealed four additional minor conformers of lower populations each, with structures of β-hairpin with type I, type II′, and type VIII β-turn, and coil with α-helix;[27] 91% of the molecular dynamics conformers had some type of β-turn and 61% had a type I β-turn. Also, the molecular dynamics data showed that confor-

* Corresponding authors. D.M.: phone, 951-827-2696; e-mail, dmorikis@engr.ucr.edu. J.D.L.: phone, 215-746-5765; e-mail, lambris@mail.med.upenn.edu.
† University of California.
‡ These authors contributed equally to the work.
§ University of Pennsylvania.

10.1021/jm0495531 CCC: $30.25
Published on Web 12/14/2004

mational interconversion in compstatin was possible with small motions of the backbone on the order of 0.1−0.4 Å and involved free energy barrier crossing of 2−11 kcal/mol.[27]

An early inhibitory activity study using an alanine scan allowed for structure−activity correlations and showed that the disulfide bridge, Val3 of the hydrophobic cluster, and the β-turn were essential for activity.[25] The same study showed that the residues before and after the β-turn, Val4 and His9, were candidates for further optimization. Specifically, Val4Ala replacement produced an analogue with slightly lowered activity and His9Ala replacement produced an analogue with slightly increased activity.[25] Follow-up inhibitory activity and NMR studies showed that acetylation of the amino-terminus produced an analogue, Ac-compstatin, with 3-fold increased activity.[18,23,28] It was first hypothesized and then shown that the removal of this charge strengthened the hydrophobic cluster and increased the activity of compstatin.[5,23] Follow-up NMR studies showed that active acetylated analogues in which His9 and/or Val4 were replaced by Ala retained the conformation with the type I β-turn, albeit at slightly altered population.[28] These analogues were Ac-H9A-NH_2, with 2-fold higher activity than Ac-compstatin (4-fold higher activity than compstatin), and Ac-V4A/H9A/T13I-NH_2, with equal activity as Ac-compstatin (or 3-fold higher activity than compstatin). Other analogues were designed with the goal to either enhance or disrupt the major structural components of compstatin. These analogues were synthesized and subjected to NMR and inhibitory activity studies, which showed that while the disulfide bridge, the hydrophobic cluster, and the β-turn were necessary for activity, the presence of all three of them was sufficient for activity.[28] In addition, the NMR and activity studies showed that the sequence of compstatin had propensity for turn formation and while both Trp and Phe at position 7 preserved the β-turn, only the analogue with Trp7 was active. This was attributed to the capability of the indole amide of the Trp side chain to form a hydrogen bond with a suitable acceptor at the binding site of C3.[28]

The NMR data provided a structural template[25] and structure−activity correlations using NMR data provided a sequence template[28] that formed the basis of further experimental and computational combinatorial optimization in the design of active compstatin analogues. The sequence template was Ac-Xaa1-[Cys2-Val3-Xaa4-Gln5-Asp6-Trp7-Gly8-Xaa9-Xaa10-Xaa11-Cys12]-Thr13-NH_2.[4,5,23,29,30] The experimental combinatorial design was based on the design of a new phage-displayed random peptide library, where only residues Xaa were randomized.[23] The experimental combinatorial design showed for the first time that an aromatic residue at position 9 was capable of producing an analogue with 2-fold higher activity than Ac-compstatin (or 4-fold higher activity than compstatin).[23] This was the analogue Ac-I1L/H9W/T13G-NH_2. In addition, the experimental combinatorial design showed that an aromatic residue at position 4 was capable of producing an active clone, albeit at lower activity than compstatin.[23] The computational combinatorial design showed even more impressive results with the prediction of several active analogues, five of which were confirmed experimentally.[29,30] In all five analogues an aromatic residue was identified at position 4 and in 2 of them an aromatic residue was also identified at position 9.

It has been clear from the rational design studies (structure- and NMR-based),[28] the experimental combinatorial design studies (phage-displayed random peptide library-based),[23] and the computational combinatorial design studies (based on a novel algorithm)[29,30] that besides Trp7 of the β-turn (residues 5−8), aromatic residues flanking the β-turn at positions 4 and 9 are important for increased activity.

In this study we report the introduction of fused-ring non-natural amino acids at position 4 and helix promoters Ala and Abu at position 9. We have performed NMR studies on selected active analogues and a molecular dynamics study to understand the effects of amino acid replacements on the structure of the analogues. The goal of our study was to determine the role of the aromaticity of the residue at position 4 and the role of a helix promoter at position 9 in the structural stability of compstatin and to make structure−activity correlations. This is the first study in which we incorporate non-natural amino acids, other than D-amino acids, in our design of compstatin analogues.

Materials and Methods

Abbreviations. Ac, acetyl group; Cha, cyclohexylalanine; Dht, dihydrotryptophan; Yphs, phosphotyrosine; 2Igl, 2-indanylglycine; Bta, β-3-benzothienyl-L-alanine; Bpa, 4-benzoyl-L-phenylalanine; 1Nal, 1-naphthylalanine; 2Nal, 2-naphthylalanine; Abu, 2-α-aminobutyric acid; IC_{50}, concentration at 50% inhibition; NMR, nuclear magnetic resonance; TOCSY, total correlation spectroscopy; NOE, nuclear Overhauser effect; NOESY, NOE spectroscopy.

Peptide Synthesis. Compstatin and its analogues were synthesized on an Applied Biosystems 433A peptide synthesizer (Foster City, CA) on either Fmoc-amide resin, 4-(2′,4′-dimethoxyphenyl-fmoc-aminomethyl)phenoxy resin (Novabiochem, San Diego, CA), or pre-loaded Fmoc-HMP resins (ABI, Foster City, CA). Using standard Fmoc protocols.[31] The following amino acids were obtained from Novabiochem: Ile, Cys(Acm), Val, Gln(Trt), Asp(OtBu), Trp(Boc), Gly, Ala, His(Trt), Arg(Pmc), Thr(tBu), Cha, Y(phs), and Abu. Bpa was obtained from Bachem (Torrance, CA), Bta was obtained from Anaspec (San Jose, CA), and 1Nal, 2Nal, 2Igl, and Dht were obtained from Advanced Chemtech (Louisville, KY).

Peptides were *N*-acetylated by treating them with 0.5 M acetic anhydride, 0.125 M DIEA, and 0.015 M hydroxybenzotriazole (ABI). Peptide disulfide cyclization was performed on resin using a 1.5 M excess of thallium(III) trifluoroacetate (Aldrich, Milwaukee, WI) in DMF (Fisher, Pittsburgh, PA).[32] Peptide deprotection and cleavage was performed using (87.5:5:2.5) trifluoroacetic acid (TFA) (ABI), phenol (Fisher), water, and triisopropylsilane (Aldrich), for 3 h at room temperature. The reaction mixture was filtered through a fritted funnel, precipitated with cold ether (Aldrich), and pelleted by centrifugation at 4 °C. Pellet was washed three times with cold ether, dissolved in 50% acetonitrile/0.1% TFA, and lyophilized. Crude peptides were dissolved in 50% TFA and purified by C18 RP-HPLC (Vydac 218TP 2.5 × 25 cm) (Vydac, Hesperia, CA) using a 5−70% acetonitrile containing 0.1% TFA gradient on a Waters 600E HPLC system (Milford, MA). Peptide purity was determined by analytical RP-HPLC and the mass was confirmed by matrix-assisted laser desorption mass spectrometry (MALDI) on a Micromass Tofspec 2E (Waters).[33] Formation of the disulfide bond in each peptide was confirmed by MALDI-TOF using a mass shift assay that involves reaction of free thiols with *p*-hydroxymercuriobenzoic acid.[34]

Inhibition of Complement Activation. Microtiter wells (NUNC) were coated with 50 μL of 1% ovalbumin (Sigma, St.

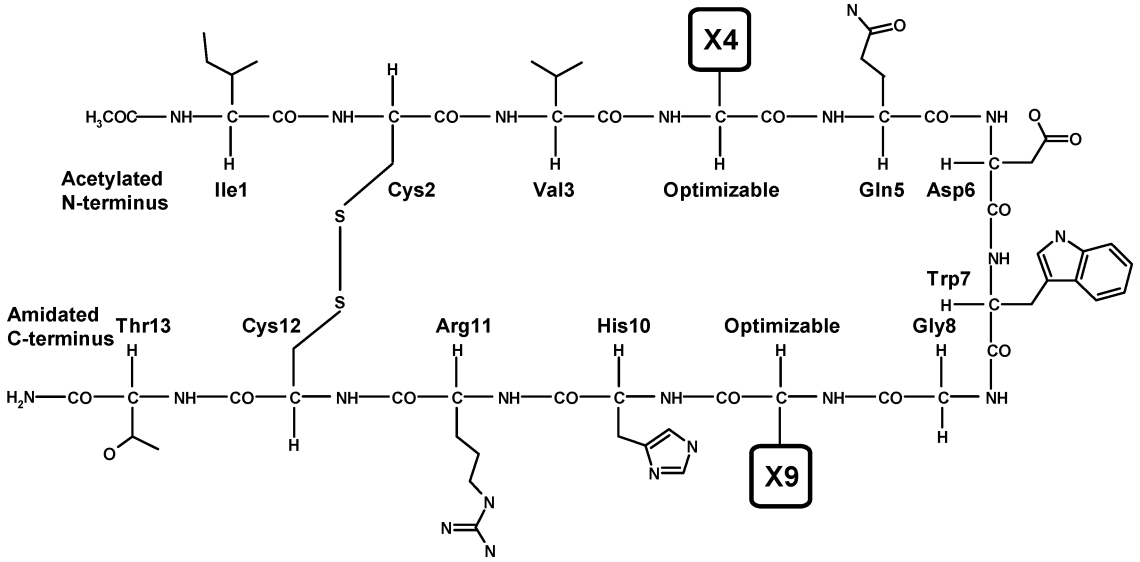

Figure 1. Representation of the chemical structure of compstatin with the optimized amino acid replacements at positions 4 and 9 indicated by X4 and X9, respectively. The figure was created using the program ISIS/DRAW (MDL Information Systems, Inc.).

Louis, MO) in PBS pH 7.4 for 2 h at room temperature. Wells were then blocked with 200 μL of 1% BSA (Sigma, St. Louis, MO) in PBS for 1 h at room temperature and then incubated with α-ovalbumin PoAb in 1% BSA/PBS 1:1000 dilution for 1 h at room temperature. Plates were washed three times with PBS/0.005% Tween 20 (Fisher), 200 μL/well. Water (30 μL) was placed in all except the first row. Peptides were solubilized in water, and the pH was adjusted to 7.4 using 0.1 N NaOH. Peptide concentration was determined using the absorbance at 280 nm and ϵ_{280}. For Ac-compstatin and Ac-V4W/H9A-NH_2, the concentrations were further confirmed using quantitative amino acid analysis. For each of the peptides that have 2Nal, 2Igl, Bta, or Dht, the concentration was determined solely on the basis of quantitative amino acid analysis[35] performed at the W. M. Keck Foundation Biotechnology Research Laboratory at Yale University. Extinction coefficient at 280 nm used for Bpa was 6826.67 and for 1Nal was 3936.12 (Mustafa O. Guler, personal communication). Peptide solutions (60 μL) were placed in the first row and then serially diluted (30 μL). Human plasma (30 μL) collected with Lipiridin[36] and diluted 1:80 in 2XGVB++ was added to each well. 2XGVB++ consisting of 10 mM barbital, 150 mM NaCl, 1 mM $MgCl_2$, 0.3 mM $CaCl_2$, and 0.2% gelatin (all from Sigma). Plates were incubated for 30 min at room temperature, washed three times with PBS pH 7.4, 0.05% Tween (PBS-T), and then incubated with 50 μL/well of goat α-human C3 HRP conjugated antibody (ICN Cappel, Costa Mesa, CA) diluted 1:2000 in 1% BSA/PBS for 1 h at room temperature. Plates were then washed three times with PBS-T. Complement fixation indicating activation was detected by addition of HRP substrate [0.05% ABTS (Roche, Indianapolis, IN) in 0.1 M sodium citrate, pH 4.2] and read at 405 nM. Percent inhibition was normalized by considering 100% activation equal to activation occurring in the absence of peptide.

Biotransformation. To assess the stability of Ac-V4W/H9A-NH_2 to proteolytic cleavage, 20 μg of peptide in 20 μL of water (pH 7.4) was incubated with 20 μL of human plasma (collected with lipirudin)[36] at room temperature and at 37 °C. Samples were diluted 1:1 with 0.1% TFA and centrifuged through a 5K cutoff filter (Millipore, Bedford, MA). The filtrate was analyzed by RP-HPLC on a C18 Column (Waters). Peak areas were determined and compared from the 0 and 24 h time points.

NMR. All four analogues studied by NMR were acetylated at the amino-terminus and amidated at the carboxy-terminus. The NMR samples were prepared in 90% H_2O and 10% D_2O buffer containing 50 mM potassium phosphate and 100 mM potassium chloride. The sample pH was ~6.0. The peptide concentrations were 3.1 mM for Ac-V4W/H9A-NH_2 and 2.1 mM for Ac-V4(2Nal)/H9A-NH_2, Ac-V4(2Igl)/H9A-NH_2, and Ac-V4W/H9(Abu)-NH_2. NMR spectra were collected at 5 °C. Analogues Ac-V4W/H9A-NH_2 and Ac-V4W/H9(Abu)-NH_2 were highly soluble and remained soluble during the NMR experiments. The analogue Ac-V4(2Nal)/H9A-NH_2 was not fully dissolved and there was always a milky suspension in the solution. The analogue Ac-V4(2Igl)/H9A-NH_2 was dissolved quickly, but some precipitation was observed after the NMR experiments.

NMR spectra were collected using a Varian Inova 500 MHz triple axis gradient spectrometer. TOCSY and NOESY spectra were collected for all analogues and DQF−COSY for the Ac-V4W/H9A-NH_2 analogue only using standard pulse sequences.[37] NOESY spectra were collected with 150 and 300 ms NOE mixing times for the Ac-V4W/H9A-NH_2 analogue and with 150 ms mixing time for the rest. TOCSY spectra were collected with 60 ms mixing time.

Spectral processing, analysis, and plotting were performed using NMRPipe/NMRDraw[38] and NMRView.[39] Solvent deconvolution was applied to all spectra in the time domain. NOESY spectra were processed with Lorentz-to-Gauss transformation window function for apodization in t_2-dimension and cosine bell squared function in t_1-dimension. The first point of the FID was multiplied by 0.5 in both dimensions of the NOESY spectra. Cosine bell apodization function was used both in t_2- and t_1-dimensions for TOCSY data. Zero-filling was applied to all spectra in both t_2- and t_1-dimensions by doubling the data size. Baseline correction was applied to all spectra after the second Fourier transform. The spectra were referenced using the known chemical shift of the H_2O resonance at 5 °C.

Molecular Dynamics Simulation. We performed a 5-ns molecular dynamics simulation for the Ac-V4W/H9A-NH_2 analogue. Because of the lack of a three-dimensional structure, we used the lowest energy structure of parent peptide compstatin[25,27] to construct a theoretical mutant with the Val4Trp and His9Ala replacements and with addition of the acetyl group at the N-terminus. This theoretical analogue was subsequently subjected to 300 steps ABNR gradient minimization before molecular dynamics to relax the possible unfavorable atomic contacts and geometric strain. Then 5 ns MD simulation was performed using the Verlet algorithm implemented in CHARMM (version c28b1) coupled with generalized Born implicit solvation. The dynamic trajectory was saved every 10 ps to a total of 500 snapshots.

Results

Our efforts focused on the residues at positions 4 and 9 of compstatin (Figure 1), which were found to be

Table 1. Names, Sequences, and Activities of Compstatin Analogues with Natural Amino Acid Replacements at Positions 4 and 9 and Comparison to Parent Peptides Compstatin, Ac-compstatin, and Ac-H9A-NH_2

no.	analogue name	sequence[a]	IC_{50} (μM)[b]	rep[c]	RIA[d]
I[e]	compstatin[f]	I[CVVQDWGHHRC]T-NH_2	53.6	8	1
II[e]	Ac-compstatin[f]	Ac-I[CVVQDWGHHRC]T-NH_2	18.1	32	3
III[e]	Ac-H9A-NH_2	Ac-I[CVVQDWGAHRC]T-NH_2	12.4	13	4
IV	Ac-V4T-NH_2	Ac-I[CVTQDWGHHRC]T-NH_2	68.3	6	1
V	Ac-V4S-NH_2	Ac-I[CVSQDWGHHRC]T-NH_2	50.9	6	1
VI	Ac-V4H-NH_2	Ac-I[CVHQDWGHHRC]T-NH_2	10.5	7	5
VII	Ac-V4F-NH_2	Ac-I[CVFQDWGHHRC]T-NH_2	10.2	6	5
VIII	Ac-V4Y/H9A-NH_2	Ac-I[CVYQDWGAHRC]T-NH_2	3.8	3	14
IX	Ac-V4W/H9W-NH_2	Ac-I[CVWQDWGWHRC]T-NH_2	3.1	6	17
X	Ac-V4W-NH_2	Ac-I[CVWQDWGHHRC]T-NH_2	2.2	7	24
XI	Ac-V4W/H9A	Ac-I[CVWQDWGAHRC]T	2.0	12	27
XII[e]	Ac-V4W/H9A-NH_2	Ac-I[CVWQDWGAHRC]T-NH_2	1.2	55	45

[a] Brackets denote cyclization through a disulfide bridge. [b] Mean IC_{50} value. [c] Rep, experimental repetition number. [d] RIA, relative inhibitory activity compared to parent peptide compstatin (analogue **I**). [e] Analogues studied by NMR: **I**, Morikis et al.;[25] **II**, Soulika et al.;[23] **III**, Morikis et al.;[28] **XII**, this work. [f] Compstatin and Ac-compstatin are amidated at the C-terminus. The amide blocking group (NH_2) is implicit with their names, in agreement with our previous publications.

Table 2. Names, Sequences, and Activities of Compstatin Analogues with Non-Natural Amino Acid Replacements at Positions 4 and 9

No	Analogue name	Sequence[a]	IC_{50} (μM)[b]	Rep[c]	RIA[d]
XIII	Ac-V4(Cha)/H9A	Ac-I[CV(Cha) QDWG A HRC]T	47.8	6	1
XIV	Ac-V4(Dht)/H9A	Ac-I[CV(Dht) QDWG A HRC]T	10.2	3	5
XV	Ac-V4(Yphs)/H9A/T13I-NH_2	Ac-I[CV(Yphs) QDWG A HRC]I-NH_2	9.6	2	6
XVI[e]	**Ac-V4W/H9(Abu)-NH_2**	**Ac-I[CV W QDWG(Abu) HRC]T-NH_2**	**1.5**	**10**	**36**
XVII	Ac-V4(2Igl)/H9A	Ac-I[CV(2Igl) QDWG A HRC]T	1.5	4	37
XVIII[e]	**Ac-V4(2Igl)/H9A-NH_2**	**Ac-I[CV(2Igl) QDWG A HRC]T-NH_2**	**1.4**	**5**	**39**
XIX	Ac-V4(Bta)/H9A	Ac-I[CV(Bta) QDWG A HRC]T	0.8	7	65
XX	Ac-V4(Bta)/H9A-NH_2	Ac-I[CV(Bta) QDWG A HRC]T-NH_2	0.8	5	64
XXI	Ac-V4(Bpa)/H9A	Ac-I[CV(Bpa) QDWG A HRC]T	1.1	6	49
XXII	Ac-V4(Bpa)/H9A-NH_2	Ac-I[CV(Bpa) QDWG A HRC]T-NH_2	0.6	6	86
XXIII	Ac-V4(1Nal)/H9A	Ac-I[CV(1Nal) QDWG A HRC]T	1.8	4	30
XXIV	Ac-V4(2Nal)/H9A	Ac-I[CV(2Nal) QDWG A HRC]T	1.4	8	38
XXV[e]	**Ac-V4(2Nal)/H9A-NH_2**	**Ac-I[CV(2Nal) QDWG A HRC]T-NH_2**	**0.5**	**10**	**99**

[a] Brackets denote cyclization through a disulfide bridge. [b] Mean IC_{50} value. [c] Rep, experimental repetition number. [d] RIA, relative inhibitory activity compared to parent peptide compstatin (analogue **I** in Table 1). [e] Analogues studied by NMR (this work) are in bold.

amenable to sequence, structure, and activity optimization.[4,5,23,28−30] Table 1 shows a series of analogues with aromatic residues (Phe, Tyr, Trp), His, Thr, and Ser at position 4 and Ala or Trp at position 9. Comparison with parent peptides compstatin, Ac-compstatin, and Ac-H9A-NH_2 is presented in Table 1. The combination of Val4Trp and His9Ala replacements in Ac-V4W/H9A-NH_2 (analogue **XII** in Table 1) yielded an impressive 45-fold higher inhibitory activity than compstatin (analogue **I** in Table 1). Upon removal of the NH_2-block of the C-terminus that leaves the backbone of this residue negatively charged, the activity dropped nearly by a factor of 2 (analogue **XI** in Table 1). This is in agreement with our previous working model that the presence of charge at the termini disrupts the functional hydrophobic cluster.[5,23,28] Figure 2 shows representative plots of percent inhibition values as a function of peptide concentration for selected analogues of Table 1, including parent peptides compstatin and Ac-compstatin.

Since the most active analogue of Table 1 involved a Trp at position 4 and an Ala at position 9 (analogue **XII**), we initiated a new design effort by introducing fused-ring amino acids at position 4 and an unbranched single-methyl amino acid at position 9 (Figure 3). The fused-ring amino acids contain one or two six-member rings or one six-member and one five-member ring; they are cyclohexylalanine (Cha), dihydrotryptophan (Dht), phosphotyrosine (Yphs), 2-indanylglycine (2Igl), β-3-benzothienyl-L-alanine (Bta), 4-benzoyl-L-phenylalanine (Bpa), 1-naphthylalanine (1Nal), and 2-naphthylalanine (2Nal). The unbranched single-methyl amino acid at position 9 is 2-α-aminobutyric acid (Abu). Ala and Abu are promoters of helical structure.[40,41] The difference between Abu and Ala is that in Abu there is a methylene spacer between its backbone and its methyl group.

Twelve of the 13 analogues have higher inhibitory activities than the parent peptide compstatin, and one has about the same inhibitory activity as compstatin (Table 2). The most active analogue, Ac-V4(2Nal)/H9A-NH_2, has an impressive 99-fold higher inhibitory activity than compstatin (analogue **XXV** in Table 2). This is currently the most active analogue of compstatin. Analogues **XVII**−**XXII** and **XXIV**−**XXV** were synthesized with and without the C-terminus block NH_2 (Table 2). It turns out that the NH_2 block of the C-terminus contributes significantly to the inhibitory activity of the most active analogues **XXII** and **XV** (Table 2). This may be the case for all analogues, but compensatory effects owed to their side chain composition cannot be excluded. Figures 4 and 5 show representative plots of percent inhibition values as a function of analogue concentration

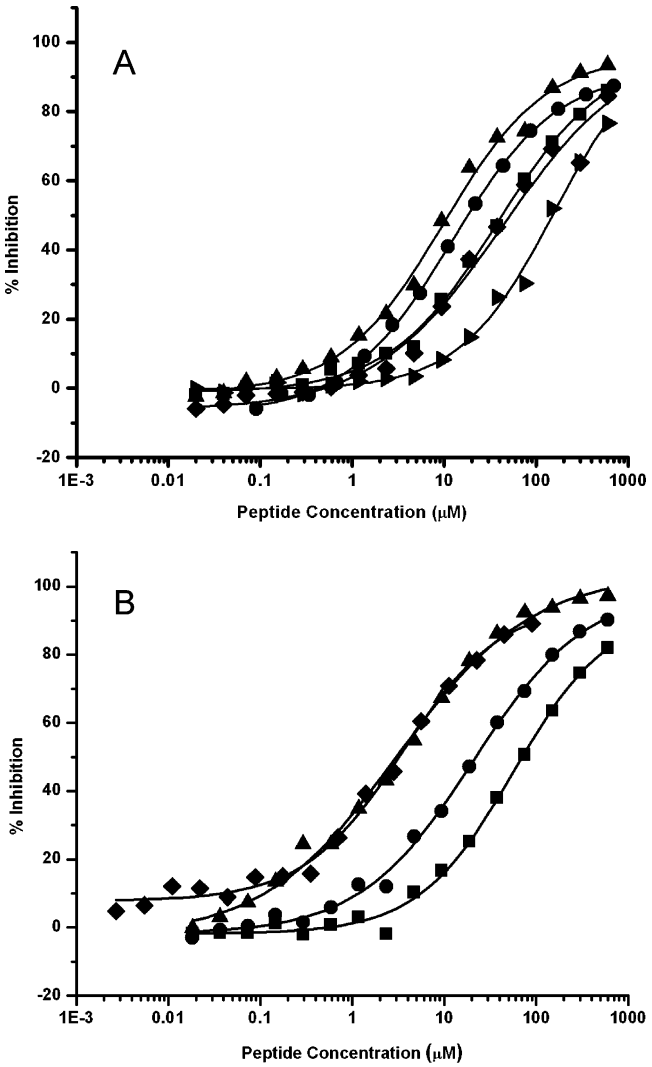

Figure 2. Plots of percent inhibition against peptide concentration for selected analogues from Table 1. These are representative plots from several experimental repetitions (Table 1). (A) Analogues with single substitutions are compared with parent peptide Ac-compstatin (circles): Ac-V4S-NH_2 (triangles pointing right), Ac-V4H-NH_2 (squares), Ac-V4F-NH_2 (diamonds), Ac-V4W-NH_2 (triangles). (B) Analogues with double substitutions are compared with compstatin (squares) and Ac-compstatin (circles): Ac-V4Y/H9A-NH_2 (triangles), Ac-V4W/H9W-NH_2 (diamonds).

for selected analogues of Table 2, including parent peptides compstatin and Ac-compstatin.

The data in Table 2 demonstrate that Trp or fused-ring non-natural amino acids at position 4, in combination with Ala or Abu at position 9, are responsible for the up to 99-fold increase in complement inhibitory activity. This is in agreement with earlier breakthrough studies using combinatorial computational design, which showed that introduction of aromaticity at position 4 had caused up to 16-fold increased activity.[29,30]

We selected four representative analogues to perform NMR studies, with the aim to understand structure−activity correlations. The selected analogues are Ac-V4W/H9A-NH_2 (**XII** in Table 1), and Ac-V4(2Nal)/H9A-NH_2, Ac-V4(2Igl)/H9A-NH_2, and Ac-V4W/H9(Abu)-NH_2 (**XVI**, **XVIII**, and **XXV** in Table 2). The rationale for the selection was the following. The peptide Ac-V4W/H9A-NH_2 is the most active analogue that consists of natural

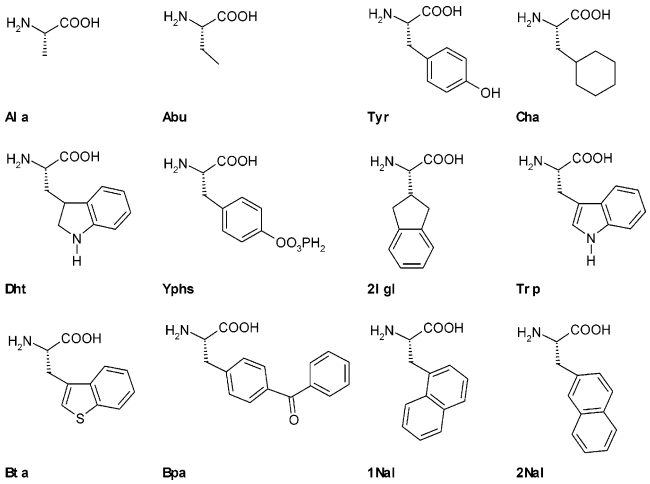

Figure 3. Structures of the amino acid replacements at positions 4 or 9 of compstatin from the analogues of Table 2. The amino acids are Ala, alanine; Abu, 2-α-aminobutyric acid; Tyr, tyrosine; Cha, cyclohexylalanine; Dht, dihydrotryptophan; Yphs, phosphotyrosine; 2Igl, 2-indanylglycine; Trp, tryptophan; Bta, β-3-benzothienyl-L-alanine; Bpa, 4-benzoyl-L-phenylalanine; 1Nal, 1-naphthylalanine; 2Nal, 2-naphthylalanine. The figure was created using the program ISIS/DRAW (MDL Information Systems, Inc.).

amino acids, with 45-fold higher inhibitory activity than compstatin (**XII** in Table 1). The side chain of Trp consists of a methylene group, an aromatic six-member ring, and an indole five-member ring (Figure 3). The analogue Ac-V4(2Nal)/H9A-NH_2 is the most active analogue to date, with 99-fold higher inhibitory activity than compstatin (**XXV** in Table 2). The side chain of 2Nal consists of a methylene group and two aromatic six-member rings, which lack hydrogen-bond capability (Figure 3). The non-natural amino acid 2Igl in the analogue Ac-V4(2Igl)/H9A-NH_2 resembles the ring structure of Trp, but is missing the potential hydrogen-bond donor indole amide and a β-methylene group (Figure 3). The NMR study of these three analogues is expected to shed light on the effect of aromaticity at position 4 on the structure of compstatin. The analogue Ac-V4W/H9(Abu)-NH_2 has Abu at position 9 that is a helix promoter, as is Ala. The side chain of Abu consists of a methylene and a methyl group (Figure 3). The NMR study of this analogue is expected to clarify a previous proposal that there is a helical propensity in the sequence and structure of compstatin.[27,28] Figure 4 shows a comparison of the percent inhibition values of these four analogues with those of parent peptides compstatin and Ac-compstatin.

NMR spectra of the four analogues are shown in Figures 6, 8, and 9. Figure 6 shows portions of the TOCSY spectra that demonstrate the identification of all 13 spin systems for each of the four analogues Ac-V4W/H9A-NH_2, Ac-V4(2Nal)/H9A-NH_2, Ac-V4(2Igl)/H9A-NH_2, and Ac-V4W/H9(Abu)-NH_2 (**XII**, **XVI**, **XVIII**, **XXV** in Tables 1 and 2). Figure 7 shows plots of the H^{α} and H^{N} chemical shift differences of theses analogues from Ac-compstatin. Figure 7 also identifies the chemical shift differences among the four analogues **XII**, **XVI**, **XVIII**, **XXV**, demonstrated by the scattering of the data points. These plots distinguish the residues whose backbone has been most affected by the replacements at positions 4 and 9. Differences owed to the replacements at positions 4 and 9 are noticeable for the H^{α}

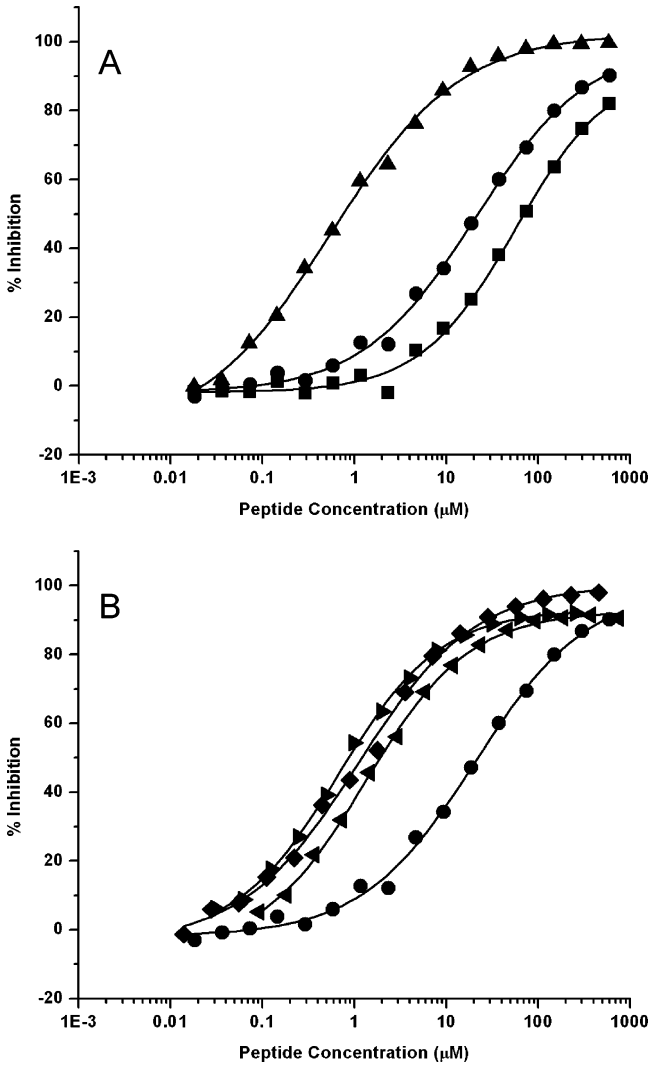

Figure 4. Plots of percent inhibition against peptide concentration for the analogues studied by NMR (Tables 1 and 2). These are representative plots from several experimental repetitions (Tables 1 and 2). (A) The analogue Ac-V4W/H9A-NH_2 (triangles) is compared to Ac-compstatin (circles) and compstatin (squares). (B) The analogues Ac-V4W/H9(Abu)-NH_2 (triangles pointing left), Ac-V4(2Igl)/H9A-NH_2 (diamonds), and Ac-V4(2Nal)/H9A-NH_2 (triangles pointing right) are compared to Ac-compstatin (circles).

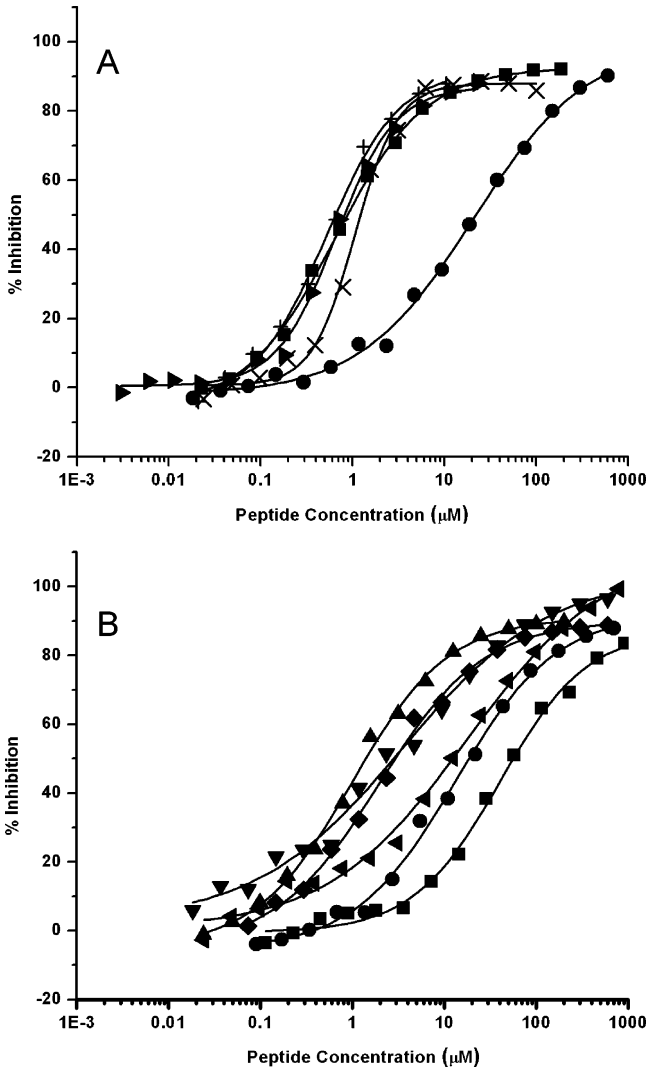

Figure 5. Plots of percent inhibition against peptide concentration for selected analogues from Table 2. These are representative plots from several experimental repetitions (Table 2). (A) Analogues with and without the NH_2 block at the C-terminus are compared with Ac-compstatin (circles): Ac-V4(Bta)/H9A (+), Ac-V4(Bta)/H9A-NH_2 (squares), Ac-V4(Bpa)/H9A (×), Ac-V4(Bpa)/H9A-NH_2 (triangles pointing right). (B) Analogues lacking the NH_2 block at the C-terminus are compared with Ac-compstatin (circles): Ac-V4(Cha)/H9A (squares), Ac-V4(Dht)/H9A (triangles pointing left), Ac-V4W/H9A (triangles pointing down), Ac-V4(1Nal)/H9A (diamonds), Ac-V4(2Nal)/H9A (triangles).

protons of Gln5, Asp6, and His10, where all analogues follow the same trend except for the Asp6 of Ac-V4(2Igl)/H9A-NH_2 (Figure 7A). The H^{α} chemical shifts of Ile1, Cys2, Val3, residue 4, Trp7, Gly8, residue 9, Arg11, Cys12, and Thr13 do not vary significantly from each other within each residue in the four analogues shown in Figure 7A. Also, noticeable differences from Ac-compstatin are observed for the H^N protons of His10, Arg11, and Cys12, where all analogues follow the same trend, and for the H^N protons of Cys2, Val3, Gln5, and Asp6, where there is scattering of the data points and no consensus trend (Figure 7B). The H^N chemical shifts of Ile1, residue 4, Trp7, Gly8, residue 9, His10, and Thr13 do not vary significantly from each other within each residue in the four analogues shown in Figure 7B.

Figures 8 and 9 show the $H^{\alpha}(\delta_1)-H^N(\delta_2)$ and $H^N(\delta_1)-H^N(\delta_2)$ regions of the NOESY spectra of the four analogues we studied. The data have been analyzed according to standard methods.[42] The backbone sequential connectivities of intraresidue $H^{\alpha}(i)-H^N(i)$ and interresidue $H^{\alpha}(i)-H^N(i+1)$ are traced in Figure 8A–D. The presence of strong $H^{\alpha}(i)$-$H^N(i+1)$ compared to $H^N(i)-H^N(i+1)$ NOEs (Figures 7 and 8) is consistent with extended conformation; but the presence of several $H^N(i)-H^N(i+1)$ NOEs is consistent with the presence of helical conformation. The latter is more obvious in the NOESY spectra of the Ac-V4(2Nal)/H9A-NH_2 and Ac-V4(2Igl)/H9A-NH_2 analogues (Figure 9B,C), in which there is better spectral dispersion that allows the identification of a nearly complete set of $H^N(i)$-$H^N(i+1)$ NOEs throughout the analogue sequences. It should be noted that all analogues Ac-V4W/H9A-NH_2, Ac-V4-(2Nal)/H9A-NH_2, Ac-V4(2Igl)/H9A-NH_2, and Ac-V4W/H9(Abu)-NH_2 (**XII**, **XVI**, **XVIII**, **XXV** in Tables 1 and 2) have better dispersion in the $H^N(\delta_1)-H^N(\delta_2)$ region

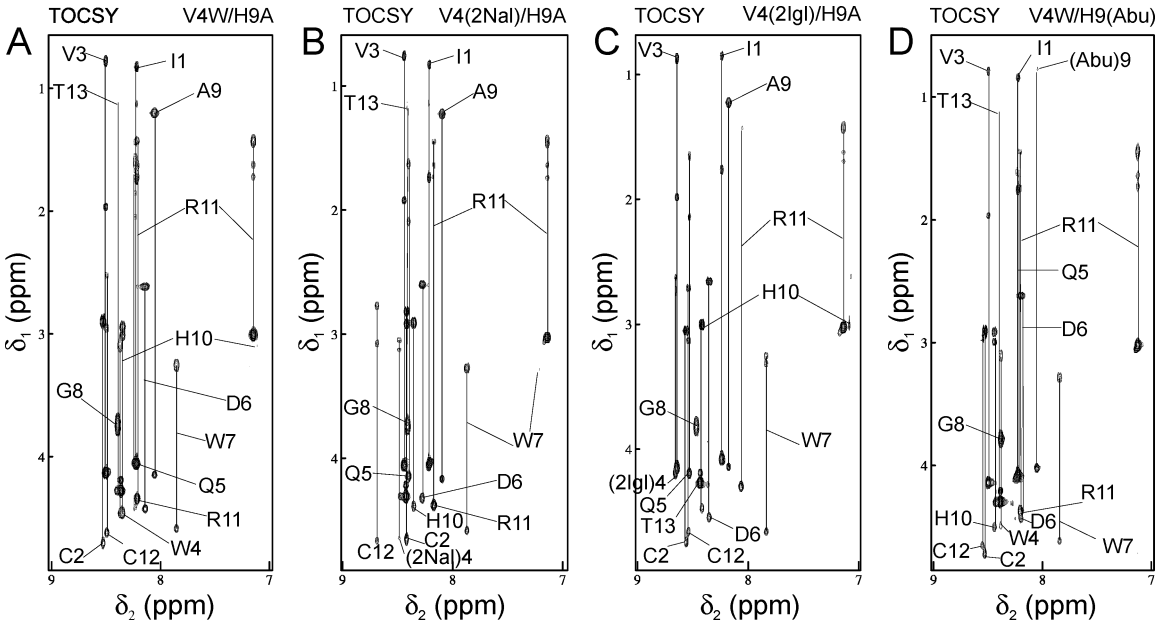

Figure 6. Portions of the TOCSY spectra depicting the backbone/side chain (δ_1)-backbone/aromatic (δ_2) region: (A) Ac-V4W/H9A-NH_2, (B) Ac-V4(2Nal)/H9A-NH_2, (C) Ac-V4(2Igl)/H9A-NH_2, (D) Ac-V4W/H9(Abu)-NH_2. The amino acid replacements are shown in the legends.

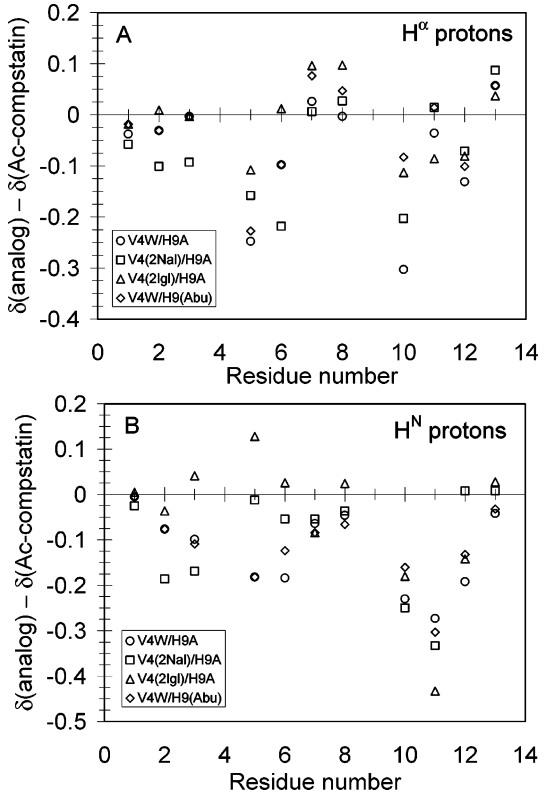

Figure 7. Plots of differences between the observed backbone chemical shifts of the four analogues of our study from the chemical shifts of Ac-compstatin: (A) H^{α} chemical shifts, (B) H^N chemical shifts. The analogues are Ac-V4W/H9A-NH_2 (circles), Ac-V4(2Nal)/H9A-NH_2 (squares), Ac-V4(2Igl)/H9A-NH_2 (triangles), and Ac-V4W/H9(Abu)-NH_2 (diamonds).

of the NOESY spectrum (Figure 9) compared to Ac-compstatin.[23] This may be attributed to the effect of ring current shift owed to the aromatic rings of Trp4, (2Nal)4, or (2Igl)4. The effect of (2Nal)4 and (2Igl)4 is expected to be stronger, because the former has two phenyl groups and the latter is closer to the backbone because of lack of β-methylene group. In combination, the NOE data suggest conformational averaging between the α- and β-regions of the Ramachandran plot. The presence of nearly equal intensity H^N(Asp6)−H^N(Trp7) and H^N(Trp7)−H^N(Gly8) NOEs (Figure 9) is consistent with a type I β-turn in the segment Gln5-Asp6-Trp7-Gly8 in all analogues, as was the case of compstatin, Ac-compstatin, and other analogues.[25,23,28] Spectral overlap prevents the observation of a weak H^{α}(Asp6)-H^N(Gly8) NOE, characteristic of a β-turn in the Ac-V4W/H9A-NH_2 and Ac-V4(2Nal)/H9A-NH_2 analogues (Figure 8A,B); however, in each of them a very weak H^{β}(Asp6)−H^N(Gly8) NOE was observed (not shown). Lack or weakness in the intensity of the H^{α}(Asp6)−H^N(Gly8) NOEs is consistent with turn flexibility, as was suggested for compstatin analogues in an earlier study by Morikis et al.[28] In the study of Morikis et al.,[28] an often weak H^{α}(Asp6)−H^N(Gly8) NOE was observable, with the aid of some spin diffusion, at higher NOE mixing times than the 150 ms used in our current study. The $H^N(\delta 1)$−$H^N(\delta 2)$ regions of the NOESY spectra (Figure 9) do not exclude the presence of additional and possibly fused β-turns.

Figure 10 shows plots of differences between the observed and random coil chemical shifts of the H^{α} protons for analogues Ac-V4W/H9A-NH_2, Ac-V4(2Nal)/H9A-NH_2, Ac-V4(2Igl)/H9A-NH_2, Ac-V4W/H9(Abu)-NH_2, Ac-H9A-NH_2, and Ac-compstatin (**XII**, **XXV**, **XVIII**, **XVI**, **III**, and **II** in Tables 1 and 2). Negative differences in the H^{α} protons are characteristic of α-helices, while positive differences are characteristic of β-sheets.[43,44] Typically, at least four consecutive residues with a negative chemical shift difference sign identify a helix and at least three consecutive residues with a positive sign identify a β-sheet. Database analysis has shown mean chemical shift difference of −0.39 ppm for helices and +0.37 ppm for β-sheets.[43,44] Otherwise, the chemical shift differences are indicative of random coil. A trend for helix formation is observed in Figure

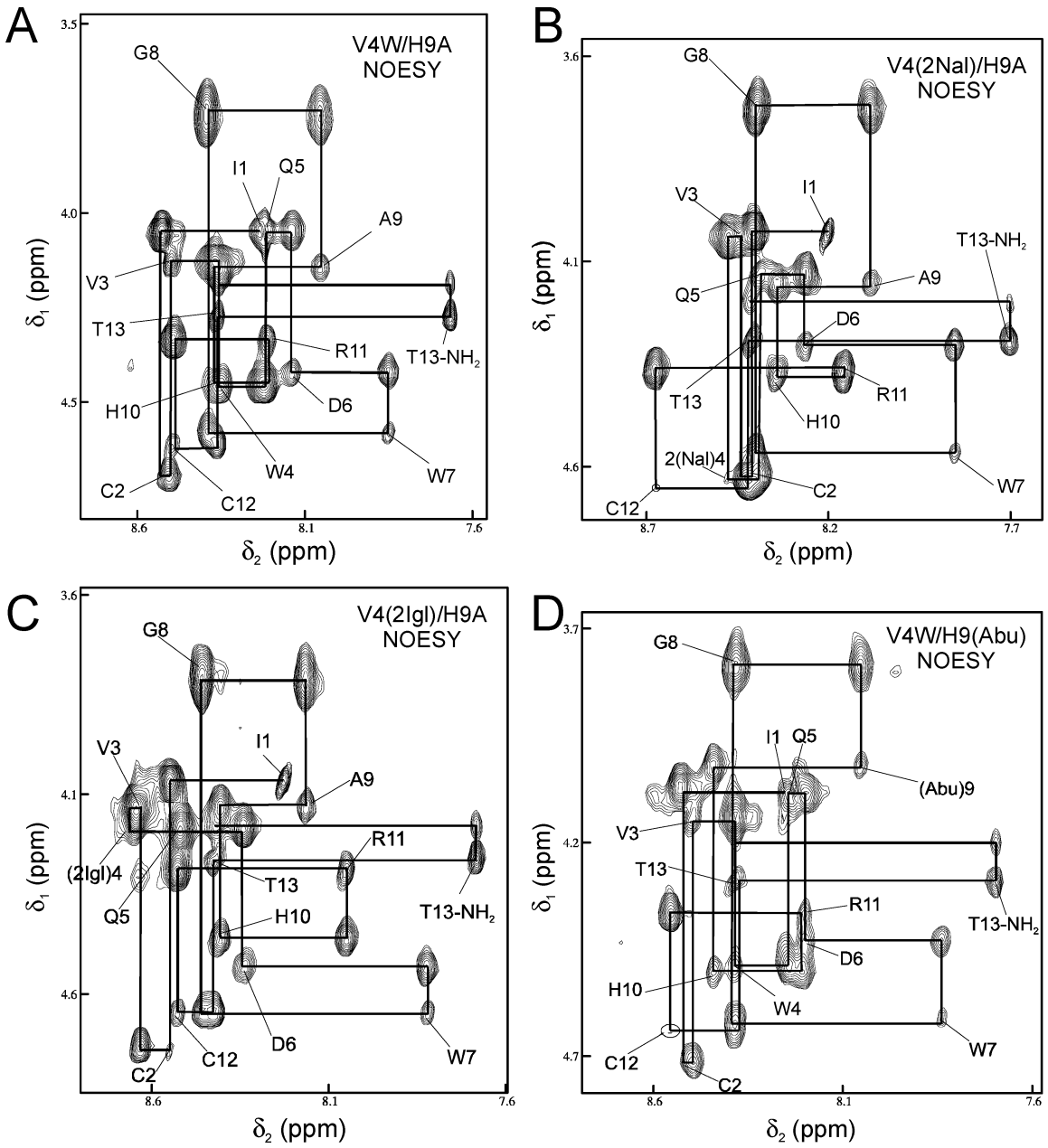

Figure 8. Portions of the NOESY spectra depicting the backbone H^{α} (δ_1)−H^{N} (δ_2) region: (A) Ac-V4W/H9A-NH_2, (B) Ac-V4-(2Nal)/H9A-NH_2, (C) Ac-V4(2Igl)/H9A-NH_2, (D) Ac-V4W/H9(Abu)-NH_2. The amino acid replacements are shown in the legends.

10 for the seven-residue segment 4−10. The mean differences are −0.16 for Ac-compstatin, −0.14 for Ac-H9A-NH_2, −0.25 for Ac-V4W/H9A-NH_2, −0.23 for Ac-V4(2Nal)/H9A-NH_2, −0.15 for Ac-V4(2Igl)/H9A-NH_2, and −0.19 for Ac-V4W/H9(Abu)-NH_2. The chemical shift differences of non-natural amino acids have not been included in the calculations, because of lack of random coil chemical shift values. These data are consistent with the promotion of weak helical conformations for residues 4−10 in analogues **II**, **III**, **XII**, **XXV**, **XVIII**, and **XVI** (Tables 1 and 2).

We have not attempted $^3J_{HN-H\alpha}$-coupling constant analysis because of the severe averaging of these parameters in small and flexible peptides and the difficulty to perform accurate measurements when the NMR lines suffer from line broadening. These difficulties have been previously discussed for peptides in general[45] and in the case of compstatin.[25]

We have searched for long-range NOEs between rings of Trp4, (2Nal)4, (2Igl)4, and Trp7, e.g., involving the indole H^{N}-proton(s) of Trp4 or Trp7 at >10 ppm, but these were absent in the spectra. Also, we searched for NOEs from ring protons of Trp4, (2Nal)4, (2Igl)4, and Trp7 with the $H^{\epsilon N}$-proton or other side chain proton of Arg11 or ring protons of His10, but these were absent as well. The lack of these NOEs from the NOESY spectra does not exclude electrostatic interactions between the π-electron system of aromatic rings or π-cation interactions. This is because the NOE data are capable of identifying through-space interactions for distances up to 5.0−5.5 Å,[42] while interactions involving the π-electron system of aromatic rings are possible for distances up to 7−8 Å for $\pi-\pi$ interactions and up to 5−6 Å for $\pi-$cation intreractions.[46−50]

We have performed a 5-ns molecular dynamics simulation for the Ac-V4W/H9A-NH_2 analogue, which al-

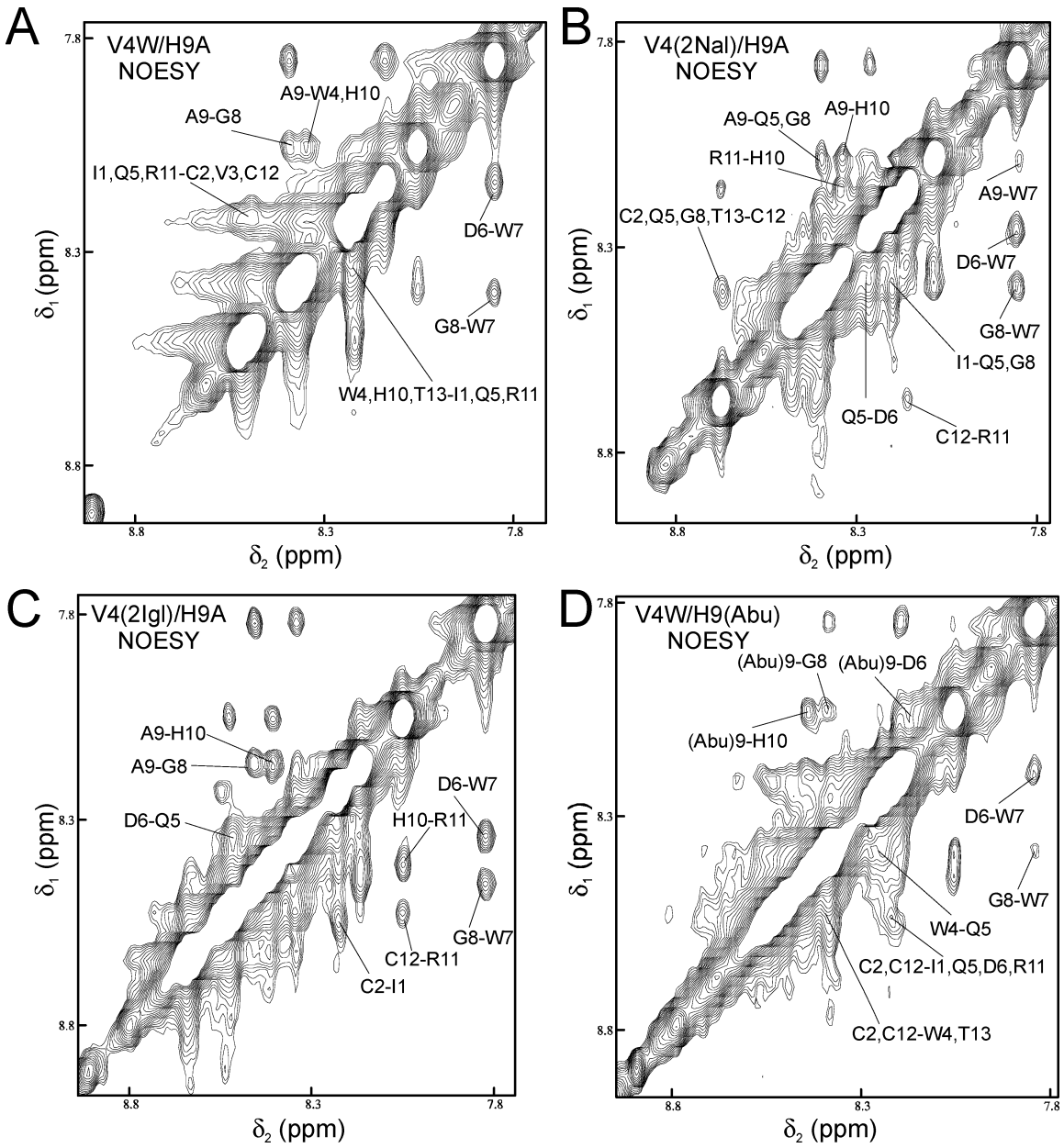

Figure 9. Portions of the NOESY spectra depicting the backbone H^N (δ_1)−H^N (δ_2) region: (A) Ac-V4W/H9A-NH_2, (B) Ac-V4-(2Nal)/H9A-NH_2, (C) Ac-V4(2Igl)/H9A-NH_2, (D) Ac-V4W/H9(Abu)-NH_2. Some cross-peaks with elongated shape represent overlapping NOEs. All possible assignments for the chemical shifts of the overlapping cross-peaks are given; however, NOEs between neighboring residues are more likely than long-range NOEs. The amino acid replacements are shown in the legends.

lowed us to look into distances longer than the NOE limit. The simulations showed interconversion among two major conformers, coil and β-hairpin, and a minor α-helical conformer. This analogue undergoes a structural transition from coil to β-hairpin at about 3 ns. Figure 11 shows the distances between the side chains of the pairs Trp4−Trp7, Trp4−His10, Trp4−Arg11, Trp7−His10, and Trp7−Arg11, which are the possible candidates for $\pi-\pi$ or π−cation interactions. Distances were evaluated using the aromatic ring centers of Trp residues, the $N^{\epsilon 2}$ of His10 and the middle point of $N^{\eta 1}-N^{\eta 2}$ atoms of Arg11. The distance of Trp4−Trp7 fluctuates mainly in the range 4−9 Å throughout the trajectory with an average value of 5.5 Å, suggesting $\pi-\pi$ interaction (Figure 11). This is further supported by a van der Waals pairwise energy stabilization for the Trp4−Trp7 pair during the simulation (data not shown). Distances suggesting π−cation interactions were not observed, except for occasional and limited visits within the proper limit (less than 6 Å) during the molecular dynamics trajectory for the side chain pairs of Trp4−Arg11 and Trp7−Arg11 (Figure 11). The remaining pairs are found at distances outside the range of $\pi-\pi$ or π−cation interactions.

For completion, we have performed a selective D-amino acid scan in the sequence of compstatin and tested for inhibitory activity (Table 3). Some of these analogues lacked Thr13 (desThr13; Table 3). One of these analogues was slightly more active (**XXXV** in Table 3) and one was 20-fold more active than compstatin (**XXXVI** in Table 3). The consensus of this study is that D-amino acids within the Cys2−Cys12 cyclic loop of compstatin disrupt the backbone structure of compstatin with the end result being the abolition of inhibi-

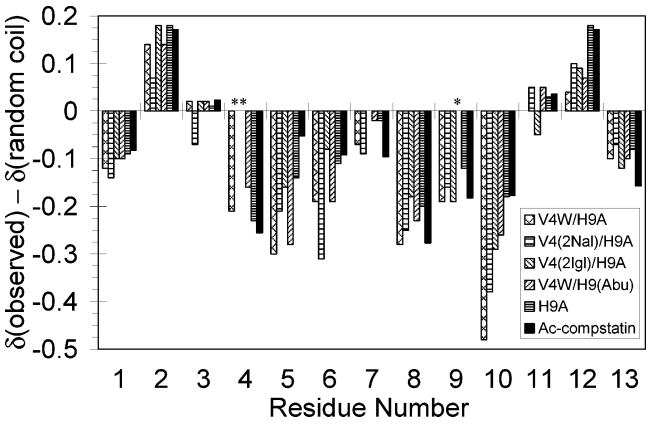

Figure 10. Plots of differences between the observed H^{α} chemical shifts of Ac-compstatin (Soulika et al.[24]) and the four analogues of our study from the H^{α} random coil chemical shift values. Random coil chemical shift values for natural amino acids are from Merutka et al.[52] Data for 2Nal, 2Igl, and Abu (marked with *) have not been included because of lack of random coil values. The analogue order (from left to right) is Ac-V4W/H9A-NH_2, Ac-V4(2Nal)/H9A-NH_2, Ac-V4(2Igl)/H9A-NH_2, Ac-V4W/H9(Abu)-NH_2, Ac-H9A-NH_2, and Ac-compstatin. The amino acid replacements are shown in the legend.

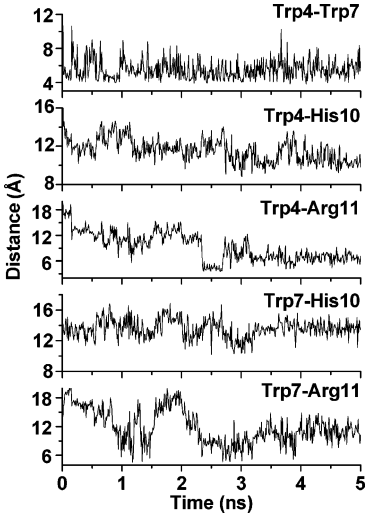

Figure 11. Plots of side chain distances representing possible intramolecular aromatic−aromatic and aromatic−cation interactions for the Ac-V4W/H9A-NH_2 analogue, derived from a 5-ns molecular dynamics simulation. The side chain pairs are marked in the panel legends. The proximity of the Trp4−Trp7 pair is indicative of π-π interaction. The remaining pairs appear to be noninteractive.

tory activity. Substitution of a D-amino acid at positions 1 and 13 does not have a significant effect on the backbone conformation of compstatin, other than contributing to the hydrophobic cluster, because these residues hang outside the cyclic loop. The backbone conformation of compstatin is dictated by the amino acids of the cyclic loop.

Discussion

We have designed 24 new analogues of compstatin that show equal or higher inhibitory activity than the parent peptide (Tables 1−3). Fifteen of these analogues contain non-natural amino acids (Table 2) or D-amino acids (Table 3). This is a continuation of our previous studies using rational design,[28] experimental combinatorial design,[23] and computational combinatorial design,[29,30] which collectively yielded peptide analogues with up to 16-fold higher inhibitory activity than compstatin (reviewed in refs 4,5). The findings of our previous studies have been the basis of the work presented here, which has yielded 15 analogues with higher than 16-fold inhibitory activities (Tables 1−3). The most active peptide analogue containing all-natural amino acids is Ac-V4W/H9A-NH_2 (**XII** in Table 1) with 45-fold higher inhibitory activity than compstatin, and the most active analogue that includes a non-natural amino acid is Ac-V4(2Nal)/H9A-NH_2 (**XXV** in Table 2) with 99-fold higher inhibitory activity than compstatin.

The main innovation in the analogues presented here is the use of fused-ring amino acids at position 4. We also tested an unbranched single-methyl amino acid, Abu, at position 9. Our choice of fused-ring amino acids was based on our previous identification of compstatin analogues containing two or three aromatic rings.[4,23,29,30] We formed the hypothesis that intramolecular $\pi-\pi$ interactions between side chains with aromatic rings or $\pi-$cation interactions involving an aromatic ring and a positively charged side chain may be contributing to the structural stability of compstatin. The candidates for $\pi-\pi$ interactions are Trp or fused-ring replacements at position 4 with Trp at position 7. The candidates for $\pi-$cation interactions are Trp or fused-ring replacements at position 4 with His10 or Arg11. To test this hypothesis and to understand the contributions of the amino acid replacements to the backbone conformation, we performed NMR studies on selected representative analogues. An additional mechanism contributing to inhibitory activity may involve intermolecular $\pi-\pi$ or $\pi-$cation interactions that contribute to the binding of the analogues to their target C3.

We have performed NMR studies for four new active compstatin analogues with optimized design at positions 4 and 9 (analogues **XII**, **XVI**, **XVIII**, **XXV**, Tables 1 and 2). These analogues include aromatic amino acids Trp, 2Nal, or 2Igl at position 4 and Ala or Abu at position 9. The incorporation of non-natural amino acids is an improvement over earlier successful rational, experimental combinatorial, and computational combinatorial optimization, which identified that positions 4 and 9, were amenable to optimization.[18,23,25,28−30] Positions 4 and 9 flank the β-turn, which comprises the segment Gln5-Asp6-Trp7-Gly8. The amino acid composition of the β-turn segment was considered optimal in previous studies.[4,5,28] Our goal was to determine the effect of the aromatic residues at position 4 and the methyl-containing residues at position 9 on the structural stability of compstatin.

Our structure evaluation protocol was based on the analysis of NMR data for the selected analogues, which were examined for consistency with previously collected NMR data of parent peptides compstatin[25] and Ac-compstatin[23] and with the predetermined three-dimensional structure and molecular dynamics simulations of compstatin.[25,27] This is an efficient protocol to study several analogues compared to the time-consuming and usually redundant structure determination (for many similar analogues) using restrained molecular dynamics-based simulated annealing methods with NMR-derived or deduced restraints. A variety of NMR spectra provide a wealth of physical observables that define

Table 3. Names, Sequences, and Activities of Compstatin Analogs with Selected D-Amino Acid and/or Position 13 Replacements

no.	analogue name	sequence[a]	IC_{50} (μM)[b]	rep[c]	RIA[d]
XXVI	Ac-V4dY/H9A/T13I-NH_2	Ac-I[CVdYQDWGAHRC]I-NH_2	>1000	2	inactive
XXVII	Ac-V4dW/H9A/T13I-NH_2	Ac-I[CVdWQDWGAHRC]I-NH_2	>1000	2	inactive
XXVIII	Ac-V4W/H9A/R11dR	Ac-I[CVWQDWGAHdRC]T	>1000	3	inactive
XXIX	Ac-Q5dQ/desT13-NH_2	Ac-I[CVVdQDWGHHRC]-NH_2	>1000	1	inactive
XXX	Ac-D6dD/desT13-NH_2	Ac-I[CVVQdDWGHHRC]-NH_2	>1000	1	inactive
XXXI	Ac-W7dW/desT13-NH_2	Ac-I[CVVQDdWGHHRC]-NH_2	>1000	1	inactive
XXXII	Ac-V3dV/V4W/H9A	Ac-I[CdVWQDWGAHRC]T	>1000	1	inactive
XXXIII	Ac-V4W/H9A/H10dH	Ac-I[CVWQDWGAdHRC]T	136.2	3	0.4
XXXIV	Ac-V4W/H9dA	Ac-I[CVWQDWGdAHRC]T	132.4	3	0.4
XXXV	Ac-I1dI/V4W/H9A	Ac-dI[CVWQDWGAHRC]T	23.1	3	2
XXXVI	Ac-V4W/H9A/T13dT	Ac-I[CVWQDWGAHRC]dT	2.7	3	20

[a] Brackets denote cyclization through a disulfide bridge. [b] Mean IC_{50} value. [c] Rep, experimental repetition number. [d] RIA, relative inhibitory activity compared to parent peptide compstatin (analogue I in Table 1).

structure, such as NOEs, NOE connectivity patterns, and NOE-derived distances, chemical shifts and chemical shift indices, *J*-coupling constants and derived specific torsion angles, and in certain instances, combination of all of the above provide deduced backbone hydrogen bonds. These physical observables, combined in the form of restraints with proper restrained computational methods, are used to determine three-dimensional structures, when needed.

Our NOE and chemical shift data of the four analogues we studied suggest conformational averaging between the β- and α-regions of the Ramachandran plot, without showing clear preference for 3_{10}- or α-helix or β-hairpin formation. Lack of $H^{\alpha}(i)-H^{N}(i+2)$, $H^{\alpha}(i)-H^{N}(i+3)$, $H^{\alpha}(i)-H^{N}(i+4)$, or $H^{\alpha}(i)-H^{\beta}(i+3)$ NOE precludes a major conformer with helical structure. Also, lack of interstrand NOEs precludes a major conformer with β-hairpin structure. It is possible that Ala and Abu at position 9 promote weak helical conformation in analogues Ac-H9A-NH_2, Ac-V4W/H9A-NH_2, Ac-V4W/H9(Abu)-NH_2, Ac-V4(2Igl)/H9A-NH_2, Ac-V4(2Nal)/H9A-NH_2 (**III**, **XII**, **XVI**, **XVIII**, **XXV**, Tables 1 and 2), as indicated by our chemical shift analysis (Figure 10). Weak helical propensity has also been indicated by chemical shift analysis for Ac-compstatin (Figure 10), in which position 9 is occupied by His. Overall, our data are consistent with the presence of a major conformer as a coil with a type I β-turn in the segment Gln5-Asp6-Trp7-Gly8, as has been the case for all active and some inactive analogues studied by NMR to date.[23,25,28] The presence of additional or fused β-turns cannot be excluded.

Our data are in agreement with previous NMR data,[23,25,28] structure determination of compstatin by NMR,[25] and molecular dynamics simulations.[27] Earlier NMR data showed evidence of averaging of NMR parameters, owed to multiple conformers[25] and flexibility.[28] NMR data of compstatin had suggested that an observable major conformer had a population of 42−63%.[25] A complete structure determination of compstatin had shown that the structure of the major conformer of compstatin was a coil with a type I β-turn.[25] Molecular dynamics simulations, based on the NMR structures, produced quantitative evidence for the presence and type of interconverting conformers and showed that the major conformer (with population 44%) was a coil with a type I β-turn,[27] in agreement with the NMR data.

In addition, a 5-ns molecular dynamics simulation for the Ac-V4W/H9A-NH_2 analogue showed the presence of two major conformers, coil and β-hairpin, and a minor α-helical conformer. Back-calculated NOE spectra using calculated backbone distances from the molecular dynamics trajectory are consistent with the presence of strong $H^{\alpha}-H^{N}$ and $H^{N}-H^{N}$ Asp6-Trp7 and Trp7-Gly8 cross-peaks and a weak $H^{\alpha}-H^{N}$ Asp6-Gly8 cross-peak. Although the weak $H^{\alpha}-H^{N}$ Asp6-Gly8 cross-peak is expected between residues 2 and 4 of a β-turn, it is not observed in the NOESY spectra, possibly owing to the choice of the NOE mixing times. Overall, the calculated data indicate the presence of a type I β-turn in the Ac-V4W/H9A-NH_2 analogue, consistent with the NMR data.

The type I β-turn together with the disulfide bridge and hydrophobic cluster have been implicated in activity of compstatin or Ac-compstatin.[4,5,18,23,25,28] Our four analogues, Ac-V4W/H9A-NH_2, Ac-V4W/H9(Abu)-NH_2, Ac-V4(2Igl)/H9A-NH_2, and Ac-V4(2Nal)/H9A-NH_2 (**XII**, **XVI**, **XVIII**, **XXV**, Tables 1 and 2), have preserved the β-turn, disulfide bridge, and hydrophobic cluster, and yet they are more active than compstatin or Ac-compstatin. We looked into additional structural elements in analogues Ac-V4W/H9A-NH_2, Ac-V4W/H9(Abu)-NH_2, Ac-V4(2Igl)/H9A-NH_2, Ac-V4(2Nal)/H9A-NH_2 (**XII**, **XVI**, **XVIII**, **XXV**, Tables 1 and 2) that may be responsible for their higher activities. Our NOE data did not show observable interaction between the aromatic rings of Trp, 2Nal, or 2Igl at position 4 and Trp7, which would have been indicative of $\pi-\pi$ interaction within each analogue. Neither did they show observable interaction between the aromatic rings at positions 4 or 7 and Arg11 or His10, which would have been indicative of $\pi-$cation interaction within each analogue. However, the NOE data are not sufficient to exclude these types of interactions. Typically NOEs are observed between protons separated by up to 5.0−5.5 Å, while $\pi-\pi$ interactions are possible for distances up to 7−8 Å[46−48] and $\pi-$cation interactions are possible for distances up to 5−6 Å.[48,49,50] NOEs in the 3.5−5.0 Å range are weak, while in the 5.0−5.5 Å range are very weak and not always observed, especially at the NOE mixing times of our experiments.[42] Intramolecular electrostatic interactions involving the π-electron system of aromatic rings may be stabilizing or structure-specific. Examination of the molecular dynamics trajectory of the Ac-V4W/H9A-NH_2 analogue allowed us to overcome the limitations of the NOESY NMR spectra. The molecular dynamics data suggested that the side chains of Trp4 and Trp7 are in distance favorable of intramolecular $\pi-\pi$ interaction.

Considering our analysis of several analogues in this study and earlier studies,[4,5,18,23,25,28−30] it is most likely

that the high activities of analogues Ac-V4W/H9A-NH_2, Ac-V4W/H9(Abu)-NH_2, Ac-V4(2Igl)/H9A-NH_2, and Ac-V4(2Nal)/H9A-NH_2 (**XII**, **XVI**, **XVIII**, **XXV**, Tables 1 and 2), all of which have Trp or fused-ring non-natural amino acids at position 4, are owed to intermolecular $\pi-$cation or $\pi-\pi$ electrostatic interactions with partners on the binding site. The same applies for the active analogues described in Klepeis et al.[29,30] that have Tyr or Phe at positions 4 and or 9. An additional role of Trp7 in activity may be that of a hydrogen-bond donor through its indole amide proton. This was proposed in an earlier study, where it was shown that Trp7Phe replacement resulted in loss of activity (Phe retains the phenyl ring but loses the amide-carrying indole ring).[28] Conclusive evidence for interactions of the aromatic residues of compstatin with partners located in the C3 binding site will be possible if a crystallographic structure of the cocrystallized β-chain of C3 with compstatin becomes available. Cation$-\pi$ interactions in ligand binding have been recently reviewed.[51]

The residues Trp4, (2Igl)4, and (2Nal)4 of analogues Ac-V4W/H9A-NH_2, Ac-V4W/H9(Abu)-NH_2, Ac-V4(2Igl)/H9A-NH_2, Ac-V4(2Nal)/H9A-NH_2 (**XII**, **XVI**, **XVIII**, **XXV**, Tables 1 and 2) contribute to the hydrophobic cluster of compstatin, which has been hypothesized to directly participate in binding to C3.[4,5,28] It is possible that the analogue Ac-V4(2Nal)/H9A-NH_2 (**XXV**, Table 2) has higher activity than Ac-V4W/H9A-NH_2 (**XII**, Table 1), Ac-V4(2Igl)/H9A-NH_2 (**XVIII**, Table 2), and Ac-V4W/H9(Abu)-NH_2 (**XVI**, Table 2) analogues because it has a double aromatic ring at 2Nal, thus enhancing the hydrophobicity of the cluster. Likewise, the double aromatic ring of 2Nal might be responsible for enhanced π-system electrostatic interaction with Trp7. The highest activity analogue presented here is Ac-V4(2Nal)/H9A-NH_2 (**XXV**, Table 2) with IC_{50} of 500 nM, 99-fold more active than compstatin.

Conclusions

In summary, we report several new active analogues of compstatin with IC_{50} values in the range of 0.5$-$50 μM. The common characteristics of these analogues are the presence of Trp or fused-ring aromatic non-natural amino acids at position 4 and single-methyl containing non-natural amino acid at position 9. The most potent analogue, Ac-V4(2Nal)/H9A-NH_2, has $IC_{50} = 0.5\ \mu$M and is 99-fold more active than parent peptide compstatin. Our NMR data (NOEs and chemical shifts) for the Ac-V4W/H9A-NH_2, Ac-V4(2Nal)/H9A-NH_2, Ac-V4(2Igl)/H9A-NH_2, and Ac-V4W/H9(Abu)-NH_2 suggest the presence of interconverting conformers, with a major conformer comprising a coil with a type I β-turn structure. The β-turn is formed from residues Gln5-Asp6-Trp7-Gly8. The β-turn is flexible, as indicated by NOEs. The aromatic residues at position 4 contribute to the hydrophobic cluster of compstatin, comprising residues Ile1-Cys2-Val3-residue 4/Cys12-Thr13. The methyl-containing residues Ala and Abu at position 9 promote the weak helical character in the segment of residues 4$-$10, as indicated by chemical shift analysis. It is likely that the aromatic residues at position 4 are involved in intermolecular electrostatic interactions with aromatic or cation partners in the binding site at C3. Our study paves the way for the incorporation of peptidomimetics in the design optimization of compstatin analogues.

Acknowledgment. We thank Dr. Dan Borchardt for help with the NMR data collection and to Ms. Charissa Wiley for technical assistance with peptide synthesis. This work was supported by the National Institutes of Health (grants GM-62134 and GM-069736) and the American Heart Association-Western States Affiliate (grant-in-aid 0255757Y).

References

(1) Lambris, J. D.; Reid, K. B. M.; Volanakis, J. E. The evolution, structure, biology and pathophysiology of complement. *Immunol. Today* **1999**, *20*, 207$-$211.
(2) Walport, M. J. Complement. Second of two parts. *New Engl. J. Med.* **2001**, *344*, 1140$-$1144.
(3) Walport, M. J. Complement. First of two parts. *New Engl. J. Med.* **2001**, *344*, 1058$-$1066.
(4) Morikis, D.; Soulika, A. M.; Mallik, B.; Klepeis, J. L.; Floudas, C. A. et al. Improvement of the anti-C3 activity of compstatin using rational and combinatorial approaches. *Biochem. Soc. Trans.* **2004**, *32*, 28$-$32.
(5) Morikis, D.; Lambris, J. D. Structural aspects and design of low-molecular-mass complement inhibitors. *Biochem. Soc. Trans.* **2002**, *30*, 1026$-$1036.
(6) Sahu, A.; Morikis, D.; Lambris, J. D. Complement inhibitors targeting C3, C4, and C5. *Therapeutic interventions in the complement system;* Lambris, J. D., Holers, V. M., (Eds.); Humana Press: Totowa, NJ, 2000; pp 75$-$112.
(7) Sahu, A.; Lambris, J. D. Complement inhibitors: A resurgent concept in antiinflammatory therapeutics. *Immunopharmacology* **2000**, *49*, 133$-$148.
(8) Morikis, D.; Sahu, A.; Moore, W. T.; Lambris, J. D. Design, structure, function and application of compstatin. *Bioactive peptides in drug discovery and design: Medical aspects;* Matsoukas, J., Mavromoustakos, T., (Eds.); Ios Press: Amsterdam, 1999; pp 235$-$246.
(9) Sahu, A.; Lambris, J. D. Structure and biology of complement protein C3, a connecting link between innate and acquired immunity. *Immunol. Rev.* **2001**, *180*, 35$-$48.
(10) Lambris, J. D., Holers, V. M. (Eds.) *Therapeutic interventions in the complement system*; Humana Press: Totowa, NJ, 2000.
(11) Morgan, B. P.; Harris, C. L. Complement therapeutics; history and current progress. *Mol. Immunol.* **2003**, *40*, 159$-$170.
(12) Makrides, S. C. Therapeutic inhibition of the complement system. *Pharmacol. Rev.* **1998**, *50*, 59$-$87.
(13) Sahu, A.; Kay, B. K.; Lambris, J. D. Inhibition of human complement by a C3-binding peptide isolated from a phage-displayed random peptide library. *J. Immunol.* **1996**, *157*, 884$-$891.
(14) Nilsson, B.; Larsson, R.; Hong, J.; Elgue, G.; Ekdahl, K. N.; et al. Compstatin inhibits complement and cellular activation in whole blood in two models of extracorporeal circulation. *Blood* **1998**, *92*, 1661$-$1667.
(15) Fiane, A. E.; Mollnes, T. E.; Videm, V.; Hovig, T.; Hogasen, K. et al. Compstatin, a peptide inhibitor of C3, prolongs survival of ex vivo perfused pig xenografts. *Xenotransplantation* **1999**, *6*, 52$-$65.
(16) Fiane, A. E.; Mollnes, T. E.; Videm, V.; Hovig, T.; Hogasen, K. et al. Prolongation of ex vivo-perfused pig xenograft survival by the complement inhibitor Compstatin. *Transplant Proc.* **1999**, *31*, 934$-$935.
(17) Soulika, A. M.; Khan, M. M.; Hattori, T.; Bowen, F. W.; Richardson, B. A. et al. Inhibition of heparin/protamine complex-induced complement activation by Compstatin in baboons. *Clin. Immunol.* **2000**, *96*, 212$-$221.
(18) Sahu, A.; Soulika, A. M.; Morikis, D.; Spruce, L.; Moore, W. T. et al. Binding kinetics, structure$-$activity relationship, and biotransformation of the complement inhibitor compstatin. *J. Immunol.* **2000**, *165*, 2491$-$2499.
(19) Furlong, S. T.; Dutta, A. S.; Coath, M. M.; Gormley, J. J.; Hubbs, S. J. et al. C3 activation is inhibited by analogues of compstatin but not by serine protease inhibitors or peptidyl alpha-ketoheterocycles. *Immunopharmacology* **2000**, *48*, 199$-$212.
(20) Mollnes, T. E.; Brekke, O. L.; Fung, M.; Fure, H.; Christiansen, D. et al. Essential role of the C5a receptor in E-coli-induced oxidative burst and phagocytosis revealed by a novel lepirudin-based human whole blood model of inflammation. *Blood* **2002**, *100*, 1869$-$1877.
(21) Klegeris, A.; Singh, E. A.; McGeer, P. L. Effects of C-reactive protein and pentosan polysulphate on human complement activation. *Immunology* **2002**, *106*, 381$-$388.

(22) Sahu, A.; Morikis, D.; Lambris, J. D. Compstatin, a peptide inhibitor of complement, exhibits species- specific binding to complement component C3. *Mol. Immunol.* **2003**, *39*, 557−566.
(23) Soulika, A. M.; Morikis, D.; Sarrias, M. R.; Roy, M.; Spruce, L. A.; et al. Studies of structure−activity relations of complement inhibitor compstatin. *J. Immunol.* **2003**, *171*, 1881−1890.
(24) Schmidt, S.; Haase, G.; Csomor, E.; Lutticken, R.; Peltroche-Llacsahuanga, H. Inhibitor of complement, Compstatin, prevents polymer-mediated Mac-1 up-regulation of human neutrophils independent of biomaterial type tested. *J. Biomed. Mater. Res. Part A* **2003**, *66A*, 491−499.
(25) Morikis, D.; Assa-Munt, N.; Sahu, A.; Lambris, J. D. Solution structure of compstatin, a potent complement inhibitor. *Protein Sci.* **1998**, *7*, 619−627.
(26) Klepeis, J. L.; Floudas, C. A.; Morikis, D.; Lambris, J. D. Predicting peptide structures using NMR data and deterministic global optimization. *J. Comput. Chem.* **1999**, *20*, 1354−1370.
(27) Mallik, B.; Lambris, J. D.; Morikis, D. Conformational interconversion in compstatin probed with molecular dynamics simulations. *Proteins-Struct. Funct. Genet.* **2003**, *53*, 130−141.
(28) Morikis, D.; Roy, M.; Sahu, A.; Troganis, A.; Jennings, P. A.; et al. The structural basis of compstatin activity examined by structure−function-based design of peptide analogues and NMR. *J. Biol. Chem.* **2002**, *277*, 14942−14953.
(29) Klepeis, J. L.; Floudas, C. A.; Morikis, D.; Tsokos, C. G.; Argyropoulos, E.; et al. Integrated computational and experimental approach for lead optimization and design of compstatin variants with improved activity. *J. Am. Chem. Soc.* **2003**, *125*, 8422−8423.
(30) Klepeis, J. L.; Floudas, C. A.; Morikis, D.; Tsokos, C. G.; Lambris, J. D. Design of peptide analogues with improved activity using a novel de novo protein design approach. *Ind. Eng. Chem. Res.* **2004**, *43*, 3817−3826.
(31) Fields, G. B.; Noble, R. L. Solid-Phase Peptide-Synthesis Utilizing 9-Fluorenylmethoxycarbonyl Amino-Acids. *Int. J. Pept. Protein Res.* **1990**, *35*, 161−214.
(32) Edwards, W. B.; Fields, C. G.; Anderson, C. J.; Pajeau, T. S.; Welch, M. J. et al. Generally Applicable, Convenient Solid-Phase Synthesis and Receptor Affinities of Octreotide Analogues. *J. Med. Chem.* **1994**, *37*, 3749−3757.
(33) Hillenkamp, F.; Karas, M. Mass-Spectrometry of Peptides and Proteins by Matrix-Assisted Ultraviolet-Laser Desorption Ionization. *Methods Enzymol.* **1990**, *193*, 280−295.
(34) Zaluzec, E. J.; Gage, D. A.; Watson, J. T. Matrix-Assisted Laser-Desorption Ionization Mass-Spectrometry—Applications in Peptide and Protein Characterization. *Protein Expression Purification* **1995**, *6*, 109−123.
(35) Sittampalam, G. S.; Ellis, R. M.; Miner, D. J.; Rickard, E. C.; Clodfelter, D. K. Evaluation of Amino-Acid Analysis as Reference Method to Quantitate Highly Purified Proteins. *J. Assoc. Official Anal. Chem.* **1988**, *71*, 833−838.
(36) Chang, J. Y. The Functional Domain of Hirudin, a Thrombin-Specific Inhibitor. *FEBS Lett.* **1983**, *164*, 307−313.
(37) Ernst, R. R.; Bodenhausen, G.; Wokaun, A. *Principles of nuclear magnetic resonance spectroscopy in one and two dimensions;* Oxford Univeristy Press: Oxford, 1990.
(38) Delaglio, F.; Grzesiek, S.; Vuister, G. W.; Zhu, G.; Pfeifer, J.; et al. NMRPipe—A Multidimensional Spectral Processing System Based on Unix Pipes. *J. Biomol. NMR* **1995**, *6*, 277−293.
(39) Johnson, B. A.; Blevins, R. A. NMRView—A Computer-Program for the Visualization and Analysis of NMR Data. *J. Biomol. NMR* **1994**, *4*, 603−614.
(40) Millhauser, G. L.; Stenland, C. J.; Hanson, P.; Bolin, K. A.; vandeVen, F. J. M. Estimating the relative populations of 3_{10}-helix and alpha-helix in Ala-rich peptides: A hydrogen exchange and high field NMR study. *J. Mol. Biol.* **1997**, *267*, 963−974.
(41) Crisma, M.; Bisson, W.; Formaggio, F.; Broxterman, Q. B.; Toniolo, C. Factors governing 3_{10}-helix vs alpha-helix formation in peptides: Percentage of C-alpha-tetrasubstituted alpha-amino acid residues and sequence dependence. *Biopolymers* **2002**, *64*, 236−245.
(42) Wuthrich, K. *NMR of proteins and nucleic acids;* Wiley-Interscience: New York, 1986.
(43) Wishart, D. S.; Sykes, B. D.; Richards, F. M. Relationship between nuclear-magnetic-resonance chemical-shift and protein secondary structure. *J. Mol. Biol.* **1991**, *222*, 311−333.
(44) Szilagyi, L. Chemical-shifts in proteins come of age. *Progress in Nuclear Magn. Reson. Spectrosc.* **1995**, *27*, 325−443.
(45) Merutka, G.; Morikis, D.; Bruschweiler, R.; Wright, P. E. NMR evidence for multiple conformations in a highly helical model peptide. *Biochemistry* **1993**, *32*, 13089−13097.
(46) Burley, S. K.; Petsko, G. A. Aromatic−aromatic interaction—A mechanism of protein-structure stabilization. *Science* **1985**, *229*, 23−28.
(47) Gervasio, F. L.; Chelli, R.; Procacci, P.; Schettino, V. The nature of intermolecular interactions between aromatic amino acid residues. *Proteins-Struct. Funct. Genet.* **2002**, *48*, 117−125.
(48) Meyer, E. A.; Castellano, R. K.; Diederich, F. Interactions with aromatic rings in chemical and biological recognition. *Angew. Chem. Int. Ed.* **2003**, *42*, 1210−1250.
(49) Burley, S. K.; Petsko, G. A. Amino-Aromatic Interactions in Proteins. *FEBS Lett.* **1986**, *203*, 139−143.
(50) Gallivan, J. P.; Dougherty, D. A. Cation-pi interactions in structural biology. *Proc. Natl. Acad. Sci. U.S.A.* **1999**, *96*, 9459−9464.
(51) Zacharias, N.; Dougherty, D. A. Cation-pi interactions in ligand recognition and catalysis. *Trends Pharmacol. Sci.* **2002**, *23*, 281−287.
(52) Merutka, G.; Dyson, H. J.; Wright, P. E. Random Coil ^{1}H Chemical-shifts obtained as a function of temperature and trifluoroethanol concentration for the peptide series GGXGG. *J. Biomol. NMR* **1995**, *5*, 14−24.

JM0495531